

# Global Journal of Science Frontier Research: I Interdisciplinary

Volume 17 Issue 1 Version 1.0 Year 2017

Type: Double Blind Peer Reviewed International Research Journal

Publisher: Global Journals Inc. (USA)

Online ISSN: 2249-4626 & Print ISSN: 0975-5896

# Parabolic Dish Concentrating Collector for Indirect Solar Cooking

By Amós Veremachi, Azher Zia, Boaventura C. Cuamba, Jorgen Lovseth & Ole Jorgen Nydal

Dhing College, Dhing, Nagaon, Assam

Abstract- Thermal performance of a point focus solar concentrating collector comprising a 2000 mm diameter, and a 665 mm focal length symmetric parabolic dish concentrator covered with reflective aluminum tiles of 0.9 reflectivity and SiC honeycomb volumetric absorber, which use atmospheric air as heat transfer fluid is experimentally investigated. The absorber was tested for two different mass flow rates. The test was intended to assess the potential of this collector as a component of solar cooker with heat storage, a prototype that has a potential to enable indirect and off-sun cooking. The prototype of a solar cooker under investigation is intended to be used in rural areas (in Mozambique) to meet multiple domestic needs in thermal energy as part of a global effort to mitigate the consequences of one of the severe problems the world faces today (desertification and deforestation), some of which are attributed to climate change.

Keywords: energy; parabolic dish; renewable sources; thermal performance; solar cooker.

GJSFR-I Classification: FOR Code: 050209



Strictly as per the compliance and regulations of:



© 2017. Amós Veremachi, Azher Zia, Boaventura C. Cuamba, Jorgen Lovseth & Ole Jorgen Nydal. This is a research/review paper, distributed under the terms of the Creative Commons Attribution-Noncommercial 3.0 Unported License http://creativecommons.org/licenses/by-nc/3.0/), permitting all non commercial use, distribution, and reproduction in any medium, provided the original work is properly cited.

# Parabolic Dish Concentrating Collector for Indirect Solar Cooking

Amós Veremachi a, Azher Zia a, Boaventura C. Cuamba a, Jorgen Lovseth a & Ole Jorgen Nydal a

Abstract- Thermal performance of a point focus solar concentrating collector comprising a 2000 mm diameter, and a 665 mm focal length symmetric parabolic dish concentrator covered with reflective aluminum tiles of 0.9 reflectivity and SiC honevcomb volumetric absorber, which use atmospheric air as heat transfer fluid is experimentally investigated. absorber was tested for two different mass flow rates. The test was intended to assess the potential of this collector as a component of solar cooker with heat storage, a prototype that has a potential to enable indirect and off-sun cooking. The prototype of a solar cooker under investigation is intended to be used in rural areas (in Mozambique) to meet multiple domestic needs in thermal energy as part of a global effort to mitigate the consequences of one of the severe problems the world faces today (desertification and deforestation), some of which are attributed to climate change. Thermal efficiency of the collector was estimated for the two mass flow rates. Preliminary results have shown that at the target temperature range the collector efficiency remained above 70 % and that the higher the mass flow rate, the lower the temperature of the air coming out of the collector.

Keywords: energy; parabolic dish; renewable sources; thermal performance; solar cooker.

# I. Introduction

xternal energy sources are an important factor for human life and development. Sufficient access to quality energy is one of the indicators of human development.

Mozambique is ranked among the countries with lowest access to electricity per capita, with only 25 % of its population connected to national electricity grid [1]. Like many other African countries, it has the majority of its population living dispersed in rural areas and depending mainly on biomass as a source of thermal energy for their multiple domestic needs. The biomass share on the country's primary energy is more than 78% [2].

Currently, however, the sources of biomass are becoming scarcer due to deforestation, changes in land use, desertification [3]-[4]. The deforestation rate in Mozambique is more than 5.6 % [5]. This reality put at risk the future of many women and children whose burden is increased due to the fact that at the present more time is required on fetching firewood to meet the families daily energy needs for cooking.

Luckily, Mozambique is among the countries with a considerable potential of renewable sources of energy. In particular, owing to the country's geographical location, the solar radiation intensity is good; with a daily annual average of  $5.2 \ kWh/m^2$  [2]-[3]-[6]. Therefore, direct collection of solar thermal energy can be an energy source for multiple domestic needs (cooking, frying, hot water, pasteurization, etc) in rural areas of Mozambique. Adoption of solar energy as a source of thermal energy also holds other indirect benefits such as an increased time availability for women and children to dedicate to their educational activities; improved in-door environment and natural environment, and less risk of burning accidents [29].

Cooking is energy intensive activity requiring medium-to-high temperatures, and thus demanding appropriate technology for harnessing and using it in an efficient way. This requirement and the low density of solar radiation at the Earth's surface turn the harvesting of this resource for cooking applications a difficult task. In direct sun, however this is possible using solar concentrators.

Over a global growing concern, on the future of conventional energy resources, solar concentrating collectors became one of the major focuses of research endeavors mainly for large scale Concentrating Solar Power applications, for more details see [7]-[8].

Currently, however there is also a growing concern over energy scarcity in small scale applications as the world witnesses the depletion of the major energy sources for people living in rural areas in developing countries. Thus, in some groups of interest small scale prototypes became a major focus of research aiming to assess their potential to benefit people in rural areas of developing countries, as a source of thermal energy for multiple domestic purposes.

Solar cooking has witnessed improvements in both research and design and deployment. In fact, solar cookers of different configurations have been suggested and some have been applied. However, the more

Author α: MSc, (PhD Candidate in Science and Energy Technology), Department of Physics, Eduardo Mondlane University-Maputo-Mozambique. e-mail: averemachi@gmail.com

Author o: MSc (Former Student at the Department of Physics-Uppsala University-Sweden). e-mail: azher.zia@gmail.com

Author p: Professor, Department of Physics, Eduardo Mondlane University-Maputo-Mozambique.

e-mail: boaventura.cuamba@gmail.com

Author  $\omega$ : Emeritus Professor, Department of Physics, Norwegian University of Science and Technology-NTNU, Trondheim-Norway.

Author ¥: Professor, Department of Energy and Process Engineering, NTNU-Trondheim-Norway. e-mail: ole.j.nydal@ntnu.no

widespread solar cooker types allow for direct cooking; in which case collection and cooking are performed simultaneously, for more details see [9]. Normally the cooking pot is placed onto focal point of the concentrator and the person performing cooking is subject to perform it under sun; facing all the potential consequences arising from excessive exposition to solar radiation.

Direct solar cookers can, however, only be used during periods of direct sun shine. Therefore, they have limited usefulness when the sun shine is intermittent due to weather conditions and cannot be used in off-sun conditions.

The intermittency of the sun shine, the risks associated with the reflected radiation and the lack of cultural acceptance, are some of the factors that have limited the use of solar cookers in Mozambique, as discussed by Otte [10].

To overcome some of the limitations of direct solar cookers, a thermal storage is essential in the solar system. Solar heat can then be collected while the sun is available and stored for later use. So, a solar stove with heat storage, which has a potential to enable indirect and off-sun cooking has be proposed.

The proposed system comprises a collector subsystem (parabolic dish solar concentrator-PDSC and absorber), heat storage (HS) and the tracking mechanism.

The collection of solar thermal energy can be done through different configurations. In one of them, the absorber can be a component part of the HS, as it was done by [11]-[12]; in which case the charging is done by direct illumination of the storage [29]. Thus the heat is absorbed at the top part of the HS and conducted through the storage medium; in the other configuration, the absorber and HS are different entities, for details see [13]-[14]-[15]. In the latter case, a heat

carrier medium is required to transport the generated heat in both charging and discharging mode.

In many applications, PDSC appears coupled with Stirling engine for electricity production purposes [16]-[17], and some studies on application of PDSC that have thermal energy as an end product for cooking purposes used oil as heat transfer fluid [18]-[19]. Meanwhile common applications of solar collectors using air as HTF are intended for space heating and crop drying [20]. Scarcely are found examples of successful applications of PDSC that use air as heat transfer fluid that are intended for collection of solar thermal energy for cooking purposes.

The performances of the components are interdependent in some way and together they determine the performance of the prototype. However, the performance of the collector subsystem is crucial and can affect the performance of the enter system. If the collector has poor performance, then the storage component becomes meaningless.

To assess the potential of PDSC collector to be used as a component of a solar cooker intended to enable indirect cooking; in this paper its thermal performance is experimentally investigated. The PDSC is coupled with Siliconized Carbide (SiC) honeycomb as absorbing material and air as heat transfer fluid (HTF). The collected heat is stored as sensible heat in a rockbed HS. The rock-bed is a two phase system comprising a solid material and HTF. During charging mode the HTF enters the storage at high temperature and as it goes through the voids gives up heat to the rocks and emerges at the exit at low temperature. As a consequence the bed temperature rises. To enable the purpose of this paper, outdoor tests were performed at Norwegian University of Science and Technology-Department of Energy and Process Engineering (NTNU-DEPE). The present paper will not include thermal analysis on the storage.

## Nomenclature:

$A_{ap} \ A_{abs}$	[m²] [m²]	Concentrator aperture area Absorber area	
C	[]	Geometric Concentration ratio	
$I_b$	[W/m²] []	Beam radiation Intensity	
$\eta_{\circ}$	[]	Optical Efficiency	
$arDelta_{th}$		Thermal Efficiency	
$\dot{Q}_u$	[W]	Usel heat rate	
$\dot{Q}_l$	[W]	Heat loss rate	
$\dot{Q}_{_{abs}}$	[W]	Heat rate generated at the absorber surface	
$\dot{m}$	[kg/s]	Mass flow rate	
$U_{_{I}}$	[W/m²K]	Overall loss coefficient	
$C_P$	[J/kgK]	Specific heat at constant Pressure	
F	Indice	Refers to fluid	
$T_{out}$	[K]	Temperature of the air leaving the collector	
Out	[K]	Average temperature at absorber surface	

Ambient temperature	
Cross-sectional area of the pipe	
Average air velocity	
Density as a function of Temperature	
Dynamic viscosity of air	
Hydraulic diameter	
Air speed through channels	
Fluid	
Thermal	
Leaving the system	
9	
Average	
Relative to absorber	
Ambient	
Optical	

### BACKGROUND INFORMATION AND H. GOVERNING EQUATIONS

Concentrating solar collectors are optical devices that concentrate low density solar radiation falling on their reflective surface onto a small area (absorber), thus turning the low energy density into high energy density. At the absorber surface, solar radiation is converted into thermal power and, due to high flux of solar radiation falling on it, high temperatures are produced and this effect can be used for different purposes including cooking.

Receivers are an integral part of any solar collector. In the context of PDSC applications, cavity receivers and volumetric receivers are the two types of receivers commonly used [21].

Witness of the relative importance of solar receivers, is the endeavor among researchers that have been focused on receiver modeling, not to name all, see for example [4]- [22] or through experiment [13]- [23]-[24].

Receivers for concentrating collectors should be designed in such a way to intercept as much reflected radiation from the concentrator as possible while at the same time ensuring that radiative heat losses from the receiver are minimized. Therefore, their size is determined by the compromise between intercepted radiation maximization, and heat loss from the receiver minimization to enable maximum power at sufficient temperatures for the intended application [22]. For high temperature applications, solar absorbers should have high temperature stability [16].

Consonant to these requirements, performed experimental investigation of heat losses from a small cavity receiver, using simulated solar heat source and a Synthetic Schlieren technique for flow pattern visualization out of the cavity. In addition to this, numerical modeling of convective heat losses from the receiver through CFD analysis was carried out for positive angles.

In their turn [18] designed, fabricated, studied and compared the performance of three different receivers (Volumetric Flash-VF, Volumetric Box-VB and conical tube-CT) using a PDSC designed to charge the HS. The receivers were designed to use oil as HTF. One of their findings suggested that the CT was appropriate for the concentrator due to its high thermal efficiency compared to the others, for a given flow rate.

Using air as HTF, [13] investigated the thermal performance of two similar flat solar absorbers made of different materials (stainless steel fiber wire mesh and SiC honeycomb) in a small scale PDSC. Their findings point out that HTF temperature and flow rates correlate negatively, while efficiency and flow rates correlate positively. In either case, the stainless steel absorber had a good performance as compared to honeycomb absorber.

Another study on the thermal performance of a point-focus PDSC was done by [25]. A cylindrical receiver intended for hot water or steam generation applications was used. The purpose was to find the optimal operating temperature and the impact of environmental conditions on heat loss mechanisms of the external receiver under windy conditions and in different facing directions of the blackened absorber. Their findings confirmed the well-known strong effects of absorber wall temperature, wind velocity and direction and ambient air temperature on total heat loss from the absorber.

The attainment of high temperatures in solar concentrating collectors is directly connected to the concentration ration of the collector. This notion relates the aperture area of a solar collector with the area of its absorber. Concentrator aperture area  $A_{\!ap}$  is the area of the collector that intercepts solar radiation. The concentration ratio C is the ratio between aperture area of the concentrator and the absorber area,  $A_{abs}$ :

$$C = \frac{A_{ap}}{A_{abs}} \tag{1}$$

Not all the solar radiation incident onto the concentrator surface is intercepted and captured by the absorber. The optical efficiency  $\eta_a$  is the ratio of the energy absorbed by the absorber to the energy incident on the concentrator surface.

$$\eta_o = \frac{\dot{Q}_{abs}}{A_{ap} I_b} \tag{2}$$

The ratio between the power incident at the absorber surface and the power received by the concentrator is a function of many factors (e.g. the ability of the tracking mechanism to keep the optical device accurately aligned with the sun, optical properties of the reflective surface and the nature (perfect or imperfect) of the concentrator geometry.

Again, not all the energy absorbed at the absorber surface is converted into useful energy. The high energy density at the absorber surface gives a high temperature. Therefore, temperature gradients between absorber and ambient arise and become a driving force for heat losses; the absorber becomes hotter than the surrounding components and ambient. As such, heat losses may occur in different modes (conductive, convective and radiative). The ability of the absorber to minimize heat losses is connected to thermal efficiency of the absorber. Thermal efficiency of the absorber is given by the following expression:

$$n_{abs} = \frac{\dot{Q}_u}{\dot{Q}_{abs}} \tag{3}$$

This parameter accounts for all types of thermal losses from the surface where heat is generated.

From formula (3), an alternative expression for useful heat can be obtained as follow:

$$\dot{Q}_u = \eta_{abs} \dot{Q}_{abs} = \eta_o \eta_{abs} A_{ap} I_b = \eta_{th} A_{ap} I_b \quad (4)$$

In the expression above  $\eta_{\it th} = \eta_{\it o} \eta_{\it abs}$  is the overall efficiency of the collector for the optical to thermal conversion.

Energy balance equation formulated at the absorber can be written as:

$$\dot{Q}_{abs} = \dot{Q}_u + \dot{Q}_l \tag{5}$$

 $\dot{Q}_{\mu} = (\dot{m}.c_{P})_{f}.(T_{out} - T_{in})$ Where (6)

$$\dot{Q}_{l} = A_{abs} \cdot U_{l} \cdot \left(T_{av} - T_{a}\right) \tag{7}$$

In the above equation  $U_i$  is the overall heat loss coefficient. Solving for  $Q_u$ , the following expression is strait forward:

$$\dot{Q}_{u}=\dot{Q}_{abs}-\dot{Q}_{l}=\eta_{o}A_{ap}I_{b}-A_{abs}U_{l}\left(T_{av}-T_{a}\right) \tag{8}$$

To characterize the thermal performance of a solar concentrating collector, the concept of thermal efficiency is used. This concept refers to the ratio between useful energy carried by the HTF and the energy falling onto concentrator aperture:

$$\eta_{th} = \frac{\dot{Q}_u}{A_{av}I_{av}} = \frac{\left(\dot{m}c_P\right)_f \left(T_{out} - T_{in}\right)}{A_{av}I_{av}} = \eta_o - \frac{A_{abs}U_l}{A_{av}I_{av}} \left(T_{av} - T_a\right)$$

$$\eta_{th} = \eta_o - \frac{U_l}{\frac{A_{ap}}{A_{abs}} I_b} (T_{av} - T_a) = \eta_o - \frac{U_l}{CI_b} (T_{av} - T_a)$$
 (9)

Assuming all radiation reflected from the concentrator surface reach the absorber surface:

$$\dot{Q}_{l} = \eta_{o} A_{ap} I_{b} - \dot{Q}_{u} \Leftrightarrow A_{abs} U_{l} (T_{av} - T_{a}) = \eta_{o} A_{ap} I_{b} - \dot{Q}_{u}$$

The energy balance enables the computation of  $U_{I}$  as a function of the absorber temperature:

$$U_{l} = \frac{\eta_{o} A_{ap} I_{b} - \dot{Q}_{u}}{A_{abs} (T_{cu} - T_{s})} = \frac{\dot{Q}_{l}}{A_{abs} (T_{cu} - T_{s})}$$
(10)

#### Research Methodology III.

For the test to take place, a SiC honeycomb absorber 105 x105x105 mm<sup>3</sup> from the Chinese Company Pingxiang Zhongying Packing Co. LTD was delivered at DEPE-NTNU.

A cubic receiver housing with truncated cone terminal was prepared in Department's Lab and the Sic was inserted within the housing, see Fig.1 .In [8], advantages of SiC honeycomb absorber that favor its application in solar industry are outlined; not to name all, high temperature tolerance, thermal shock resistant and also mechanical strength are some of them.

The receiver was then mounted onto parabolic dish concentrator through a support structure that enabled it to have the lower surface to be located at the focal region of the concentrator, see Fig.2.

Then the receiver was connected to an air carrying pipe comprising stiff pipe which in turn was connected to the flexible pipe (made of 3 pieces of corrugated steel flexible pipe connected one after the other). The pipe was intended to carry the heated air from the receiver to the storage.

To monitor temperatures at the irradiated surface of the absorber and also temperature of the air leaving the absorber, 3 to 4 thermocouples were used. One at the absorber surface, 3 at different positions

along the air carrying pipe of which the first was positioned 5 cm above the upper surface of the absorber.

c

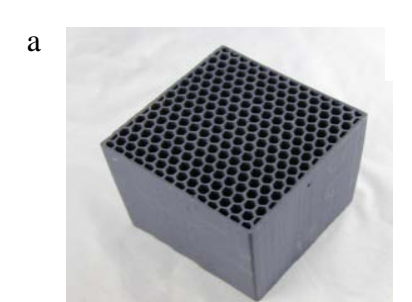






Figure 1: Showing a) SiC honeycomb absorber, b) Absorber housing and c) The receiver

Then, the absorber housing was covered with one layer of 5 mm Aerogel insulation, followed by a cover of two layers of reflective aluminum film on top. The geometric concentration ratio of the collector is 272.

Table 1: Sic honeycomb properties

Property	Values	Property	Values
Nr channels	17x14	Side wall thickness	1.3 mm
Channel dimension	7.5 mm	Specific surface area	366 m²/m³
Wall thickness	1.2 mm	Void (%)	57 %
Specific heat	750 J/kg.k	Thermal Conductivity	50-250 W/m.k

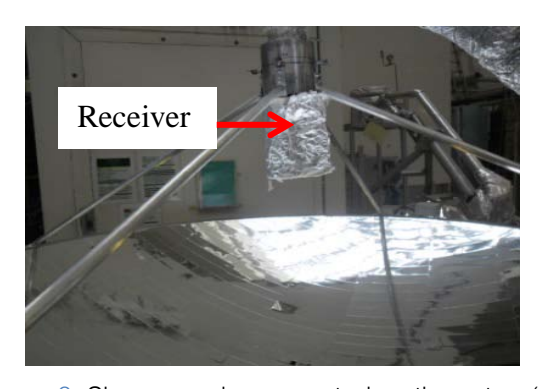




Figure 2: Shows receiver mounted on the setup (left) and irradiated receiver during tests (right)

The forced convection is generated by a fan with speed controller-P.Lemmens from air movement Company Type ESB3 Rev04-010009 connected to the HS outlet. The air speed is measured at fan outlet which has the same diameter as the air carrying pipe. Assuming no air leakage along the pipe and in steady state the air speed at the fan outlet can be used to calculate the air speed along the carrying pipe.

The average air mass flow rate is estimated through the expression (11):

$$\dot{m} = A v_{av} \rho_{av} (T) \tag{11}$$

In this expression A is the cross sectional area of the pipe,  $v_{av}$ , the average air speed (air speeds were

measured each 30 min, using a handheld  $W_{\rm M}$  Digital Anemometer DA 4000 and from the data the average was calculated);  $\rho_{av}(T)$  the average air density as a function of temperature (taken from tables of thermophysical properties of air).

The mentioned set of thermocouples was then connected to a data logger which in turn is interfaced to a PC through a labview program to log temperatures each second.

The incident beam flux was measured using a pyrheliometer at meteorological station located at the roof of Physics Department building located at the same Campus as the test location.

The following figure shows the setup used during the experiment.



Figure 3 a: Showing the heat storage and data logging system

In the first experiment, run under an average air mass flow rate of 4.4 g/s, only 3 thermocouples were used to monitor temperature of air along the pipe. The thermocouple located at the surface of the absorber had a cupper support to help fix it at the central honeycomb absorber channel. However, due to high flux density the metal was melt and the sensor did not give the readings. So,  $T_1$  is the first thermocouple measuring the temperature of air leaving the collector.

In the second test however, run under an average air mass flow rate of 5.52 g/s, another thermocouple was positioned at the absorber surface. Therefore,  $T_1$  represents reading from that thermocouple, while  $T_2$  is the temperature of air leaving the collector given by the first of 3 thermocouples along the air carrying pipe.

The pressure drop is an important parameter for the collector performance as it is a source for an informed choice of pumping power. With Reynolds number estimated at 725.5, through the small channels of the absorber the flow regime is laminar and the pressure drop can be calculated as in [26] by :

$$\Delta p = \frac{32\mu v \Delta x}{D^2} \tag{12}$$

The power required can be calculated as follow:

$$P = \frac{\dot{m}\Delta p}{\rho(T)} \tag{13}$$

# IV. RESULTS AND DISCUSSION

Figure 4 shows temperature of air leaving the collector at different points along the pipe and beam intensity at the first test.



Figure 3 b: Showing the collector sustem during the test

As can be seen from fig.4, the air leaves the collector at temperatures above 350°C during the experiment; with even high temperature between 10:19 and 11:34 probably due to high beam radiation intensity registered during this period. The sharp drops in air temperature encounter justification on weather conditions, shading of sun by clouds. This factor can be witnessed by the curve of beam radiation. Other factors are radiation loss due to imperfect focusing and increased convective heat losses.

In most of the cases, the drop in air temperature is not simultaneous with drop in beam radiation intensity. Due to thermal inertia, when beam radiation drops due to passing clouds, the absorber is still hot and hot air is pumped in; only after some time it also drops.

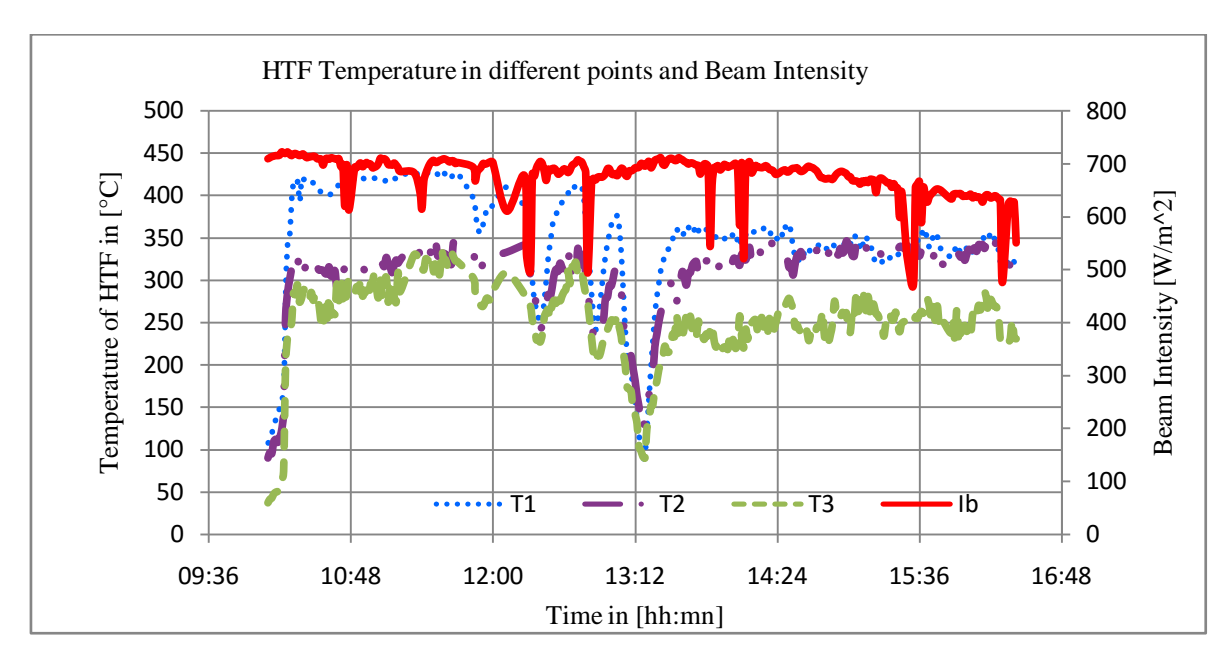


Figure 4: Showing Beam Intensity and temperature profiles of the air leaving the colector in 3 different points along the pipe during 1st experiment (9/7/2014)

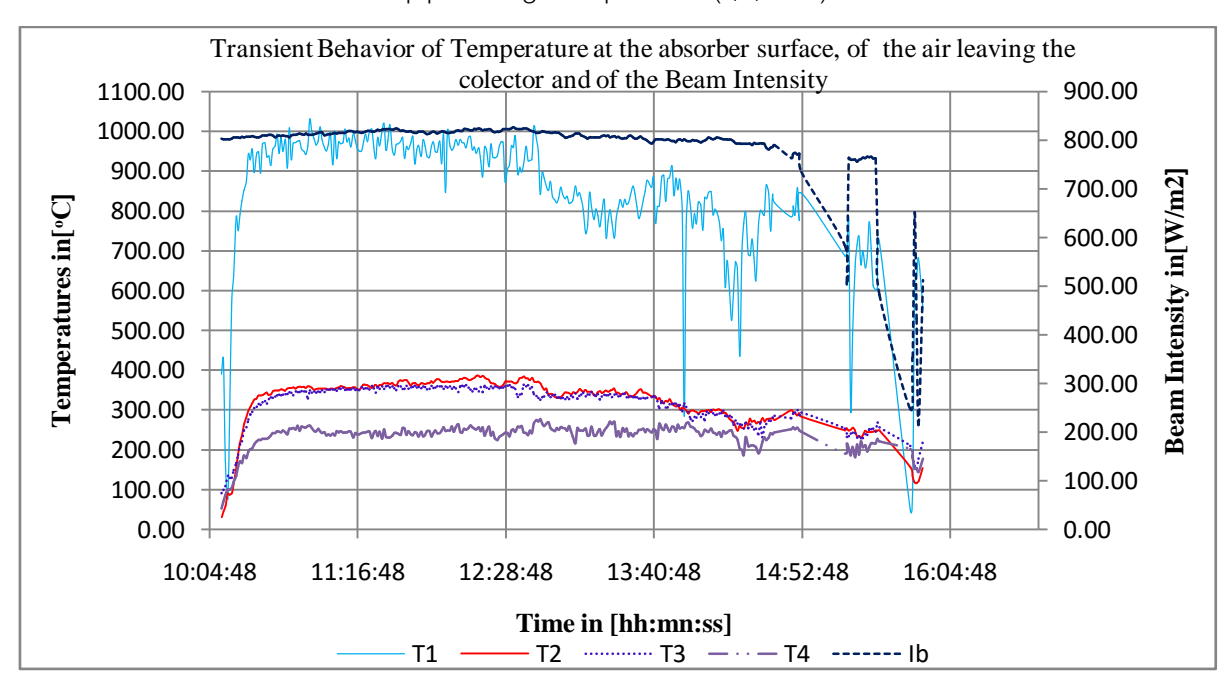


Figure 5: Showing beam radiation intensity, temperature profile at the absorber surface and of the air leaving the collector at 3 different points along the pipe during 11.07.2014 test

In figure.5, the behavior of beam radiation intensity  $I_b$ , the temperature at the absorber surface  $T_1$  and the temperature of the air along the air carrying pipe ( $T_2$  to  $T_4$ ) during second test are compared. The experiment was run under an average air mass flow rate of 5.52 g/s. This mass flow rate is almost 25% higher than the mass flow rate in the first experiment. This increase is mainly due to an increased sucking speed. The immediate consequence of an increased fan speed is less time interaction between the HTF and the absorbing material.

As can be seen from the  $I_{\rm b}$  curve, during the second test, beam intensity remained almost steadily during the major part of the test (from 10:11 hrs to 14:40 hrs), but the temperature at the surface of the absorber surface varied appreciably. These variations can be attributed to radiation loss due to imperfect focusing and convective heat losses. Despite these factors, it can be noted from the readings of the first sensor for air temperature,  $T_2$  that during this period the HTF left the collector at the temperatures above 350°C most of the time.

Figure 6 shows the behaviors of the beam radiations during the first and second tests. From this chart it can clearly be seen that the weather during the 2<sup>nd</sup> experiment was good during most of the time as compared to the 1<sup>st</sup> test. Hence, the beam radiation for the 2<sup>nd</sup> test remained stable and slightly higher than during the 1<sup>st</sup> test. However, a comparison between Fig.4 and Fig.5, reveal the effect of an increased air mass flow rate on the temperature of the air leaving the collector. This can be easily seen by the fact that

although beam radiation intensity was slightly lower in the first experiment as compared to the same quantity in the second experiment, the temperature of the air leaving the collector is lower in the second experiment.

Although there was a drop on the air temperature leaving the collector during the  $2^{\rm nd}$  test, caused by an increased mass flow rate, in both cases the HTF leaves the collector subsystem at temperatures above 350°C, suitable for cooking and frying purposes.

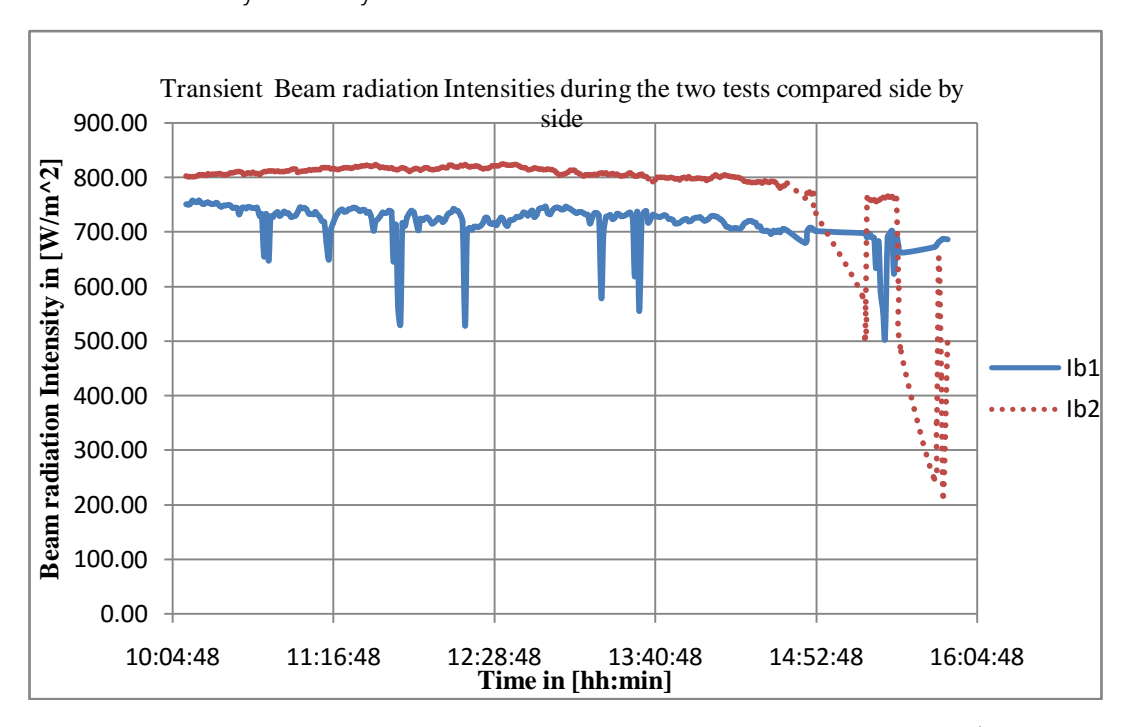


Figure 6: Charts showing the behavior of beam radiation during the 1st (09/07/2014) and 2<sup>nd</sup> (11/07/2014) tests

In figure 7, the behaviors of solar power input, the useful heat, radiative heat losses and the absorber temperature during the  $2^{nd}$  test are compared.

As can be seen from fig.7 the curve showing the behavior of radiative heat losses throughout the test is similar to the curve of the absorber temperature during the same period, as expected. The higher the absorber surface temperature, the higher the radiative heat losses become.

High temperatures were observed at the absorber surface during the test. From Stephan-Boltzmann law, radiative heat losses become pronounced at temperatures of order of  $10^2$  degrees. In our case, despite the small absorber area, radiative heat losses are expected to be dominant over other forms of heat losses owing to high temperatures at its surface, as indicated by the curve given by  $T_1$  in figure 5.

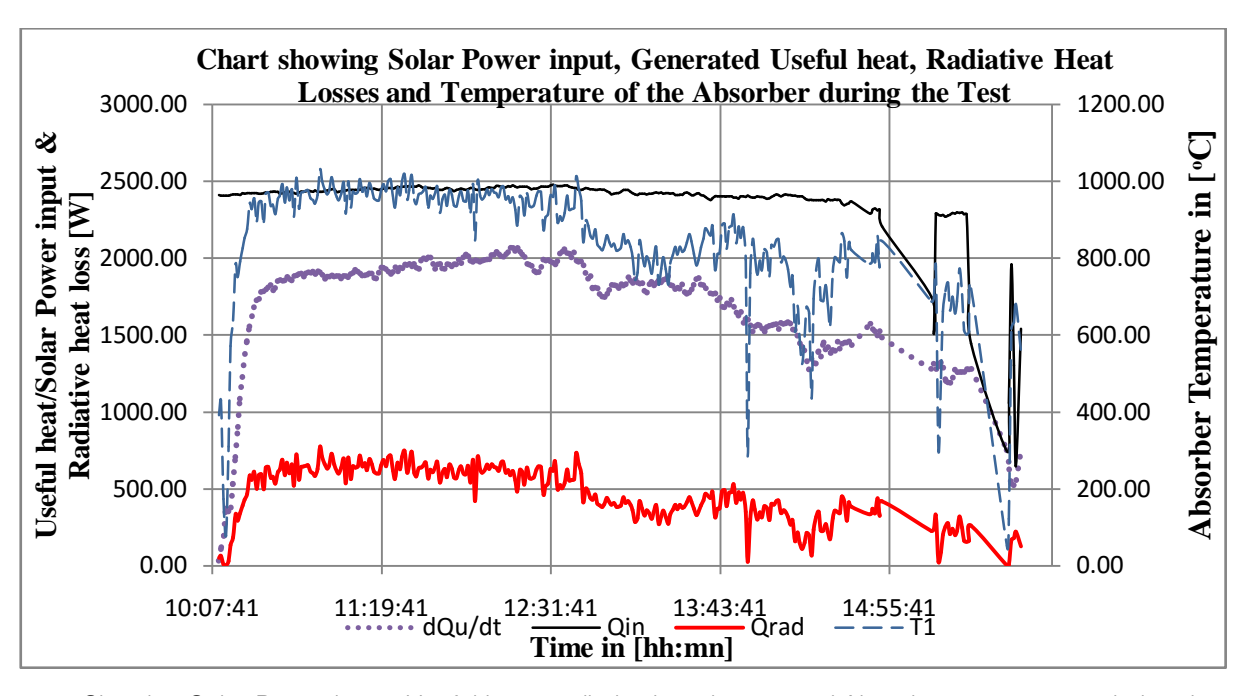


Figure 7: Showing Solar Power input, Useful heat, radiative heat losses and Absorber temperature during the test

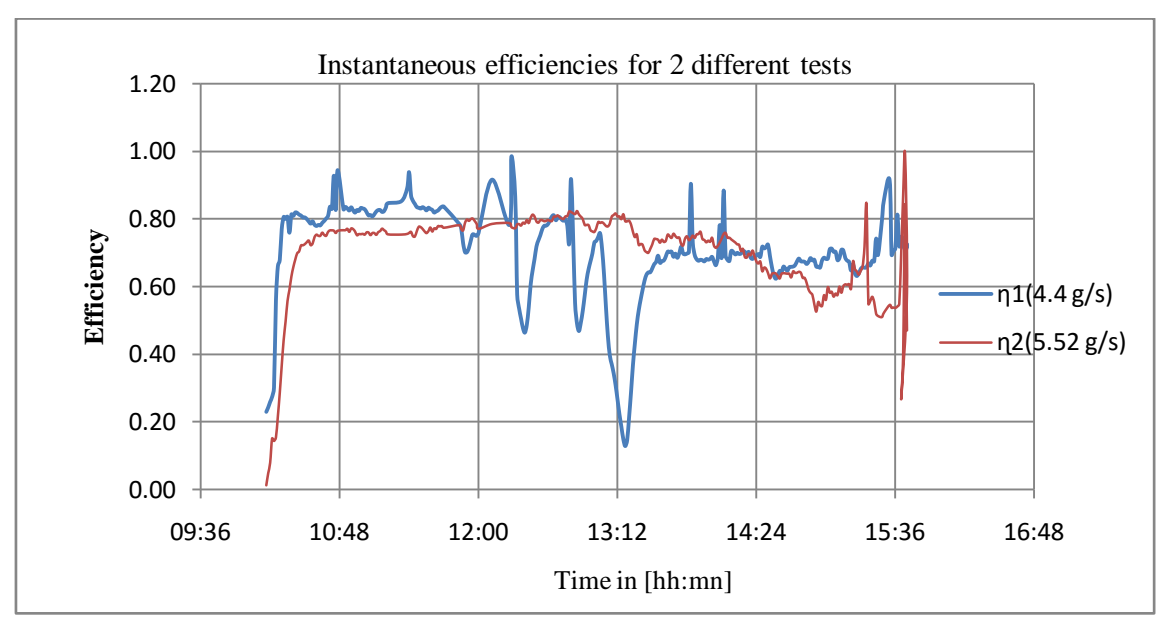


Figure 8: Showing transient instantaneous efficiencies for both tests

In figure 8 the transient behavior instantaneous efficiencies for two experiments, performed under different mass flow rates, are presented. As can be seen from the chart, the instantaneous curve for the first experiment exhibit sharp increases and sharp drops on the efficiency, while for the second test is stable between 10:15 hrs until 13:00 hrs. The behavior of the instantaneous efficiency reflects the behavior of beam intensity during the experiments. respectively. Sharp increases reflect the consequence of source obstruction by clouds and the phenomenon of thermal inertia of the absorber, as explained before. But sharp drops may reflect loss of radiation due to imperfect focusing as well as an increased wind speed.

Both factors lead to a decrease on useful heat carried by the HTF.

The solar heat is absorbed on the receiver surface, pass into the material by conduction and is then transferred to the air flow. Thus, the temperature of the surface is considerably higher than the air exit temperature, dependent on the conductivity of the absorber material and the heat transfer process. A simplified model for heat transfer will be discussed. As the radiation distribution on the receiver was not monitored, constant radiation intensity on the top was assumed. The flow through the receiver is laminar by a clear margin. This means that the heat transfer coefficient h is independent of channel air speed and

that the pressure drop is given by equation 10. The width between parallel hexagonal channel sides is 5.5 mm and  $\Delta x$  is length. Since  $\mu$  varies approximately as  $T^{2/3}$  in the actual region, v will be depressed in the hot, central region, and mass flow is reduced because of the

 $\frac{1}{T}$  temperature dependence. Temperature differences

may thus be increased during the air heating process. The temperature differences will to a certain degree be reduced by sideways heat conduction in the material, but due to the hexagonal structure, sideways conductivity is about half of the longitudinal one.

Heat transfer SiC – air is calculated assuming the same flow and temperature in all channels. With  $T_s$  &  $T_a$  representing absolute temperatures in SiC & air;  $Q_s$  heat current in SiC,  $Q_{s0}$  front surface value, the equations governing the heat transfer with the assumptions mentioned above are given in [27]:

$$Q_s = \Lambda \cdot \frac{dT_s}{dx},\tag{14}$$

 $\varLambda$  is longitudinal heat conductivity of absorber material times its total cross section. The derivation is relative to distance x from receiver surface.

$$\frac{dQ_s}{dx} = H.(T_s - T_a) \tag{15}$$

Where H=h.L , h is heat transfer coefficient and L total inside wall length of channels.

$$Q_{s0} - Q_s = J.(T_a - T_{amb})$$
 (16)

Where  $T_{amb}$  is ambient temperature,  $J = \dot{m}.c_P$  (air mass flow rate times its heat capacity).

By derivations and substitutions these equations can be converted to an equation in the variable part of T<sub>s</sub>:

$$\frac{d^2Y}{dx^2} + a.\frac{dY}{dx} - b.Y = 0$$
 (17)

Where

$$Y=T_s-T_{amb}-rac{Q_{s0}}{J}$$
 ,  $a=rac{H}{J}$  and  $b=rac{H}{\Lambda}$ 

Assuming constant coefficients, the acceptable solution of this equation is

$$Y = Y_o \cdot \exp(-\alpha x) \tag{18}$$

Where

$$\alpha = \frac{\sqrt{a^2 + 4b} + a}{2}$$

A solution to the model in [27] indicated in eqs. (14 to 17) is shown in the chart presented in Figure 9.

From this chart, the air cooling effect on the receiver with an increased mass flow rate can be noted, with the receiver presenting lower temperatures for the case of higher mass flow rate.

As discussed above, the model is based on a homogeneous heating on the top and the same air flow through all channels. The first condition is not satisfied giving also unequal flow, amplified by the fact that the viscosity of air increases with temperature, giving higher flow through the cooler parts. SiC thermal resistance is temperature dependent, and the curves in Fig. 9 are calculated using data for siliconized SiC given in [28]; 40 W/ (m.K) at 25 °C, 15 W/(m.K) at 630°C.

By using standard models as discussed e.g. in [26], we find  $\alpha=46$  and 57 m<sup>-1</sup> at absolute temperature 600 and 1000 K, respectively. This means that the 1/e-length is of the order of 2 cm for the variable Y. A value of 50 W/(m.K) was assumed for the material heat conductivity, probably a too high value. In reality, the coefficients are functions of x through  $T_a$  and  $T_s$ ; thus, we have a nonlinear equation that must be solved numerically. The model should ideally also be extended to include a realistic distribution of the focused solar radiation on the absorber surface.

The numerical solution to the equation is shown below:

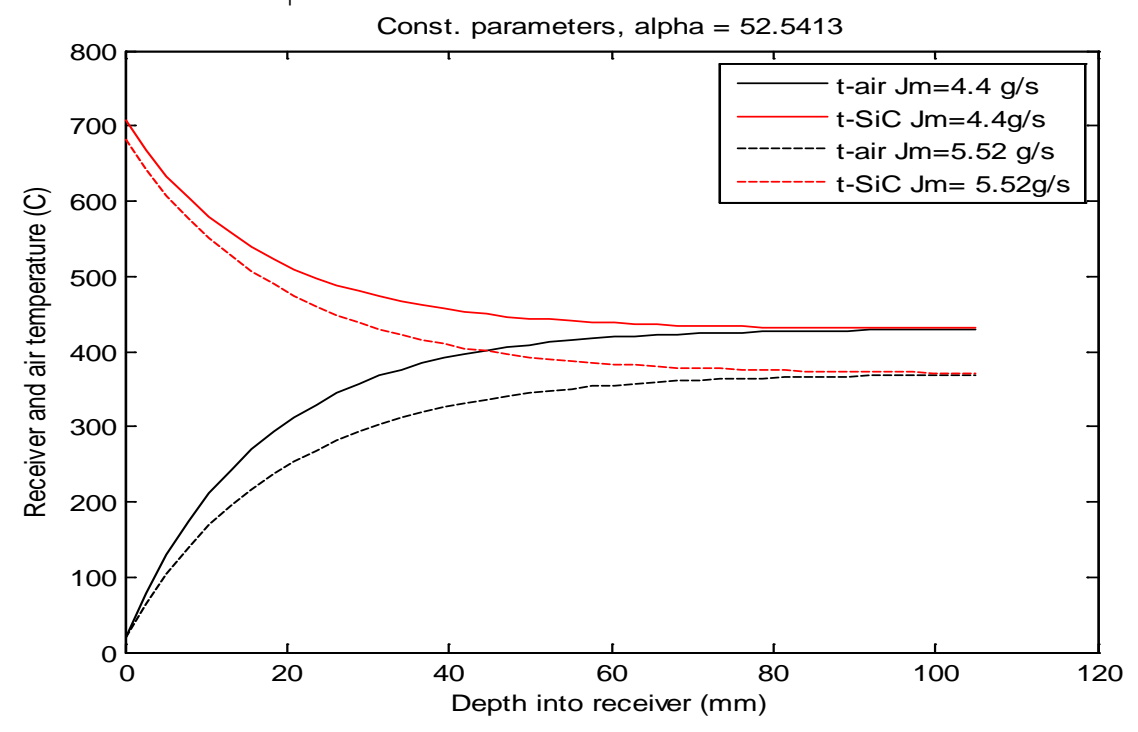


Figure 9: Modeled temperature dependence in air and receiver material to depth of the absorber for the two rates mass flow

The above discussion shows that the absorber should be as narrow as possible, still catching most of the incoming radiation. It should be made of a material with very high heat conductivity to allow transversal temperature equalization and avoid cool air an easy flow in the peripheral channels to mix with the hotter air from the inner ones. Good heat conductivity will also reduce the front temperature. A model should be made to optimize the receiver, both with respect to pumping power and heat loss.

The shape of the present receiver allows easy flow of cool air in the outer parts, and reduces mass flow of hot air in the central part, mixing at the output. This gives higher heat loss and increased pumping power for a given flow and temperature of air output.

It should be noted that for the experiments performed under the two different air mass flow rates, the transient behavior of thermal efficiency indicate a fairly good performance in both cases with the average thermal efficiency around 70 %.

Thus, the efficiencies are about the same which enables the user to choose the relevant temperature optimal for the application by selecting the air flow from the heat conservation. This evidence suggests that, Honeycomb SiC absorber, despite the economic concerns around it as compared to some of its competitor materials, holds a potential to be used as an absorber for PDSC in small scale applications like solar cooker with HS.

In the present study the overall heat loss coefficient was found to be absorber temperature

dependent as discussed in [30]. However its average value was found to be around  $51.22~W/m^2K$ . The average pressure drop through the receiver was found to be around 330.2 Pa for the first test, which implies a fan power of 4.416 W.

# V. Conclusion

Thermal performance of a point focus concentrating solar collector comprising a 2000 mm diameter parabolic dish concentrator covered with reflective aluminum tiles of 0.9 reflectivity and a focal length of 665 mm and SIC honeycomb volumetric absorber, which use atmospheric air as HTF is experimentally investigated. The absorber was tested for two different mass flow rates in order to evaluate its potential as absorber material for solar cooker prototype with HS. The results indicate that the increase in flow rate leads to decrease in the temperature of HTF. Besides, the two flow rates gave a considerable good collector thermal efficiency of around 70%. The results of this study, concerning both high temperatures and efficiency show that an air based solar cooker is possible. However, further tests are required to assure this possibility.

# Acknowledgment

The authors are thankful to:

Paul Svend sen and Marius Østnor for technical assistance during the work and Energy and Petroleum (EnP) Project. The project is part of a collaboration project on renewable energy between Norway and

and Petroleum Program.

# References Références Referencias

several African universities, under the Norwegian Energy

- 1. Electricidade de Mocambique. Annual Statistical Report, 2014.
- **IRENA** Mozambique. Renewables Readness Assessment, 2012. Available at www.irena.org.
- 3. Cuamba, B. et al. A Solar Energy Resources Assesment in Mozambique. Journal od Energy in Southern Africa. Vol 17 Nr 4, November, 2006.
- Chikukwa, A. Modelling of a Solar Stove: Small Scale Concentrating System With Heat storage. PhD Thesis. Norwegian University of Science and Technology, 2008.
- Zolho, R. Mudancas Climaticas e as Florestas em Mocambique. Amigos da Floresta/Centro de Integridade Publica, 2010.
- Nijedorogov, N.I et al. Comprehensive Study of Solar Conditions in Mozambique: The effect of Trade Winds on Solar Components. Renewable Energy Vol. 28 Nr 12, pp.1963-1983. 2003. Elsevier Science LTD.
- Glatzmaier, G. Summary Report for Concentrating Solar Power. Thermal Storage Workshop. NREL. 2011. Retreived 05/11/2013 on http://www.osti.gov /bridge.
- Agrafiotis, C.C. et al. Evaluation of Porous Silicon Carbide Monolithic Honeycomb as Volumetric Receivers/Collectors of Concentrated Solar Radiation. Solar Energy Materials and Solar Cells-91, pps 474-488, 2007. ScienceDirect. ELSEVIER. www.sciencedirect.com.
- Solar Cookers International (SCI). http://solarcooking.wikia/com/wiki/Solar Cookers-\_International\_Network\_%28Home%29
- 10. Otte, P. Limits and Possibilities of Institutional Solar Cooking in Mozambique. Proceedings of Ises Solar World Congress. Kassel. German, 2011.
- 11. Who, F.C. Experimental and Numerical Investigation of a Small Scale Double-Reflector Concentrating Solar System with Latent Heat Storage. PhD Thesis, NTNU, 2011.
- 12. Akinwale, P.F. Development of an Asynchronous Solar-powered Cooker. Master Thesis. MIT, 2006.
- 13. Madessa, H.B et al.. Investigation of Solar Absorber for Small Scale Solar Concentrating Parabolic dish. Proceedings of ISES World Congress, Kassel-Germany, 2011.
- 14. Okello, D.. Rock Bed Stove Suitable for Solar Cookers With Thermal Energy Heat Storage Systems. PhD Thesis. Makerere University-Uganda, 2012.
- 15. Mussard, M.. A Solar Concentrator with Heat Storage and Self-circulating Liquid. PhD Thesis, NTNU, 2013.
- 16. Kalogirou, S.A. Solar Thermal Collectors and Applications. Progress in Energy and Combustion Science 30, pp. 231-295. Science Direct-Elsevier, 2004.

- 17. Y., Tian & C.Y. Zhao. A review of Solar Collectors and Thermal Energy Storage in Solar Thermal Applications. Applied Energy 104(2013); pp 538-553.
- 18. Mlatho, P. & McPherson, M.. Experimental Performance of Solar Receivers Designed to Use Oil as Heat Transfer Fluid. Conference Proceedings (Ises). Kassel, 2011.
- 19. Heetkamp, R.R.J. (2002). The Development of Small Solar Concentrating Systems With Heat Storage for Rural Food Preparation. Physica Scripta. Issue Vol 2002, T97. lopscience.iop.org/1402-2002/T97
- 20. Alkilan, M.M. et al. Review of Solar air collectors with Thermal Storage units. Renewable and Sustainable Energy Reviews 15(2011); pp 1476-1490
- 21. Alvila-Marin, A.L. Volumetric receivers in Solar Thermal Power Plants with Central Receiver System Technology: A review. Solar Energy 85, pp 891-910, 2011. Science Direct. ELSEVIER. www.science direct.com.
- 22. Beltran, R. et al. Mathematical model for the study and design of a solar dish collector with cavity receiver for its application in Stirling engines. Journal of Mechanical Science and Technology, Vol. 26 Nr.10 pp. 3311-3321, 2012.
- 23. Taumoefolau, T et al.. Experimental Investigation of Natural Convection Heat Loss From a Model Solar Concentrator Cavity Receiver. Journal of Solar Energy Engineering. Vol.126, 2004.
- 24. Senthilkumar, S. et al.. Optical and thermal performance of a three-dimensional compound parabolic concentrator for spherical absorber. Sadhana Vol. 34, Part 3; pp. 369-380. Printed in India, 2009.
- 25. Gorjian, S. et al. Thermal performance of a Pointfocus Solar Steam Generating System. Proceedings of the 21st Anual International Conference of Mechanical Engineering-ISME2013, 2013.
- 26. Incropera, F. et al. Fundamentals of heat and Mass Transfer. John Willey & Sons, Inc. 2007, 6th Edition.
- 27. Lovseth, J., Veslum, T.S; and Nydal, O. Receiver for an air-based concentrating solar oven. NTNU. (To be published).
- 28. Fend, T. Hoffschmidt, B. Pitz-Paal, R. Reutter, O. Rietbrock, P., (2004). Porous materials as open volumetric receivers; experimental determination of thermophysical and heat transfer properties. Energy Vol. 29 (5-6) pp. 823-833.
- 29. Veremachi, A. et tal. PCM Heat Storage Charged With a Double-Reflector Solar System. Journal of Solar Energy Volume 2016 (2016), Article ID 907549. http://dx.doi.org/10.1155/2016/907549, Received 23 March 2016; accepted 15 June 2016
- 30. Duffie, H.A & Beckman, W.A. Solar Engineering of Thermal Processes. John Willey & Sons, 4th Edition. 2013. Canada.